

## Structure/property relationships in polystyrene–polyisobutylene–polystyrene block copolymers

Dawn M. Crawford<sup>a,\*</sup>, Eugene Napadensky<sup>a</sup>, Nora C. Beck Tan<sup>a</sup>,  
David A. Reuschle<sup>b</sup>, David A. Mountz<sup>b</sup>, Kenneth A. Mauritz<sup>b</sup>,  
Kenneth S. Laverdure<sup>c</sup>, Samuel P. Gido<sup>c</sup>, Weidong Liu<sup>d</sup>, Benjamin Hsiao<sup>d</sup>

<sup>a</sup>US Army Research Laboratory, Building 4600, Deer Creek Loop (AMSRL–WM–MA) APG, MD 21005-5069, USA

<sup>b</sup>University of Southern Mississippi, Hattiesburg, MS 39406-0076, USA

<sup>c</sup>Department of Polymer Science and Engineering, University of Massachusetts, Amherst, MA 01003-4530, USA

<sup>d</sup>Department of Chemistry, State University of New York, Stony Brook, NY 11794-3400, USA

Received 19 November 1999; accepted 20 July 2000

### Abstract

Structure/property relationships of polystyrene–polyisobutylene–polystyrene (PS–PIB–PS) triblock copolymer made by different processes were studied using dynamic mechanical analysis (DMA). The PS–PIB–PS films were composed of approximately 30% polystyrene end-blocks. Small angle X-ray scattering (SAXS) and transmission electron microscopy (TEM) confirm that a self-assembled, segregated cylindrical morphology forms in the copolymer. DMA was used as a tool to investigate the structure–property relationships in these polymers. Modified PS–PIB–PS copolymers were also characterized. Modifications of the copolymers were carried out by conversion of approximately 20 mol% of the polystyrene end-blocks to styrene sulfonic acid. The modified copolymers exhibited distinctly different thermal characteristics than the unmodified copolymers, which were most notable in the storage modulus and  $\tan \delta$  data. The presence of sulfonic acid groups disrupted the morphology and solvent sorption characteristics of the copolymers. Dynamic mechanical behavior is discussed as it relates to the morphology of the PS–PIB–PS copolymers formed via different processing methods and chemical modification. © 2001 Elsevier Science B.V. All rights reserved.

**Keywords:** DMA; Triblock copolymer; Ionomer; Sulfonation; Microstructure

### 1. Introduction

Self-assembled morphologies occur in block copolymers that are composed of thermodynamically immiscible constituent blocks. Ordered

microstructures including spheres, cylinders, or lamellae can be observed depending on the chemical composition of the blocks, sample preparation, interactions between the blocks, or by the addition of diluent [1]. Block copolymers in which an amorphous block is present as a major constituent, and a glassy block exists as a minor component, typically exhibit the solid-state properties of thermoplastic elastomers. When a portion of the polymer chain contains an ionic

\* Corresponding author. Fax: +1-410-306-0676.  
E-mail address: dcrawfor@arl.army.mil (D.M. Crawford).

group, the block copolymer is classified as an ionomer. Association of ion-rich domains occurs in ionomers, providing “physical” crosslinks that affect the block copolymer morphology and the thermal and mechanical properties [2]. This paper addresses the structure/property relationships observed in a PS–PIB–PS block copolymer as a result of ionomeric modification in the PS end-blocks.

A commercially available triblock copolymer formulation consisting of a PS–PIB–PS backbone was studied. The polymer was comprised of approximately 30% (molar) polystyrene. The thermoplastic elastomers exhibit physical properties of rubber at low temperature and melt processable thermoplastic at temperatures above the  $T_g$  of PS. This behavior results from microphase separation of the glassy PS domains that act as physical crosslinks dispersed in the rubbery PIB matrix. The fraction of PS controls the morphology that is formed in the copolymer (cylinders, lamellae, or spheres). Cylindrical morphology exists in the PS–PIB–PS triblock composed of 30% PS. Thus, the morphology formed by the PS fraction provides a channel by which molecular transport across the film can occur, while the PIB matrix provides chemical resistance. Ionomeric modification of commercially available PS–PIB–PS copolymer was performed by sulfonation. Approximately 20 mol% of the styrene monomers were converted to styrene-sulfonic acid. The modified copolymer exhibits hydrophilic character that is necessary for transport of water vapor. The polymers were characterized in their unmodified and sulfonated form utilizing a number of experimental techniques including dynamic mechanical analysis (DMA), transmission electron microscopy (TEM), small angle X-ray scattering (SAXS), sorption experiments, and gas chromatography.

## 2. Experimental

Kuraray Inc. supplied the unmodified PS–PIB–PS tri-block copolymers. The copolymers were sulfonated in a solution of dichloroethane and hexane at 50°C with acetyl sulfate. Details of the sulfonation procedure are found elsewhere [3]. The copolymers were dissolved in toluene or toluene/hexyl alcohol mixtures at a concentration of 1% and were cast into Teflon Petri dishes. Samples were identified by the rate

of solvent evaporation and designated as fast, intermediate, or slow. The fast evaporation rate involved placing the solution in the Petri dish in a hood. The solution was completely open to the atmosphere. The intermediate evaporation rate was achieved by placing an aluminum cover over the Petri dish with a hole in the cover approximately 1 cm in diameter, and placed in a hood. The slow evaporation rate was achieved by completely covering the solution with an aluminum lid and thus, the solvent evaporation was confined to the edges of the cover which were not sealed. As with all the solutions, the casting dish was placed in a hood for the duration of film formation. An ultra-fast evaporation rate was achieved by spraying a solution (5% polymer concentration) onto a substrate and allowing the film to form under a hood.

DMA was performed using an I Mass autovibron (automated Rheo-200 rheovibron, Toyo Instruments). Films of approximately 0.01 cm thickness were evaluated between  $-130$  and  $+100^\circ\text{C}$  at a heating rate of  $1^\circ\text{C}/\text{min}$ . Data were collected at 1 Hz.

Solvent absorption data were collected by submerging dry samples in HPLC grade water for specific time intervals. Weight measurements were taken until saturation was reached. Weight averages were used to calculate solubility ( $S$ ) defined as weight of liquid absorbed per weight of dry sample. Water diffusion experiments were performed using an HP5890 gas chromatograph (GC). A cylindrical fixture held the sample membrane horizontally while the top surface of the sample was flooded with HPLC grade water. The other side of the sample was swept with dry nitrogen and sent to a split injector of the GC oven equipped with a thermal conductivity detector (TCD).

TEM characterization was performed on cast samples coated with a 10 nm gold layer. A JEOL 100CX TEM microscope operated at 100 kV accelerating voltage was utilized. TEM samples were prepared by cutting 30–80 nm thick sections using a cryomicrotome, and staining in  $\text{RuO}_4$  vapors for 4 h.

SAXS was performed on beamline X27C at National Synchrotron Light Source, Brookhaven National Laboratory. Data were collected using a pinhole collimated beam and image plate detectors and were reduced by background subtraction and circular averaging. The wavelength used was 1.54 Å. The sample to detector distance was about 1000 mm.

### 3. Results and discussion

#### 3.1. DMA

The tensile storage modulus  $E'$ , loss modulus  $E''$ , and  $\tan \delta$  are plotted as a function of temperature and shown in Fig. 1.  $E'$  shows a distinct drop at the glass transition temperature ( $T_g$ ) of the PIB matrix and another decrease that begins at approximately  $93^\circ\text{C}$  associated with onset of the glass transition of the PS domains. The  $\tan \delta$  curve exhibits a low-temperature shoulder at approximately  $-60^\circ\text{C}$  that is likely a contribution from less-restricted PIB chains. The  $T_g$  of pure PIB is  $-70^\circ\text{C}$  [4]. The low-temperature shoulder appears to correspond with the peak of  $E''$ . The  $T_g$  is defined as the temperature corresponding with the maxima in the  $E''$  data and was measured at approximately  $-63^\circ\text{C}$  for the PS–PIB–PS copolymers.  $T_g$  was previously reported for noncommercial PS–PIB–PS polymers to be approximately  $-65^\circ\text{C}$  using DSC [5], which is in good agreement with the DMA data.

Variation in solvent evaporation rate did not have a significant effect on dynamic mechanical behavior. The most apparent difference was observed between films formed via the fastest evaporation rate (spraying) and the slowest evaporation (2 or 3 weeks required for

film formation). Films formed via slow evaporation exhibited slightly higher values of  $E'$ , slightly higher magnitudes of  $E''$  and  $\tan \delta$  compared to the sprayed films. These data are shown in Fig. 2a, b, and c, respectively. TEM confirmed that slow solvent evaporation rates during film formation resulted in better long-range order compared to fast evaporation rates. Cylinders formed by the glassy styrenic blocks were oriented with their axes parallel to the film plane. This morphology is consistent with the  $E'$  shown in Fig. 2a. An increase in tensile storage modulus would be expected when the glassy cylinders exist parallel to the film plane. The changes in loss properties shown in Fig. 2b and c suggest that a more disordered morphology caused by ultra-fast evaporation rates (spraying) may inhibit the microphase separation of the PS and PIB domains causing a slight reduction in  $E''$  and  $\tan \delta$  peak magnitude. This result was observed to a much greater extent following sulfonation. Kim and Libera [6,7] previously reported on the effect of solvent evaporation rate on thin film morphology of similar triblock copolymers. Control of solvent evaporation has a more profound effect on block copolymer morphology in very thin films ( $\sim 50$  nm) than in the bulk as seen in the present investigation.

Sulfonation of the PS–PIB–PS copolymer had the greatest effect on dynamic mechanical behavior.

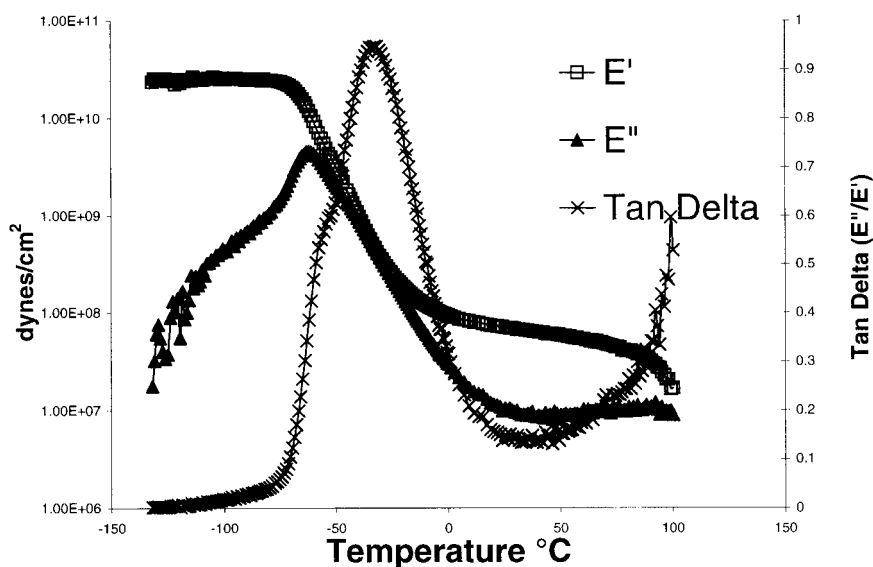


Fig. 1. DMA of unmodified PS–PIB–PS copolymer.

DMA results for PS-PIB-PS copolymers and their ionomers are shown in Fig. 3a–c. Fig. 3a shows  $E'$  plotted as a function of temperature for the two polymers. Sulfonation of the block copolymer resulted in a much higher rubbery  $E'$ . The ionomer was

observed to be more thermally stable with no indication of changes in  $E'$  at 100°C as was observed for the non-modified copolymer. The loss modulus of the two polymers is shown in Fig. 3b. These data indicate that sulfonation of the block copolymer does

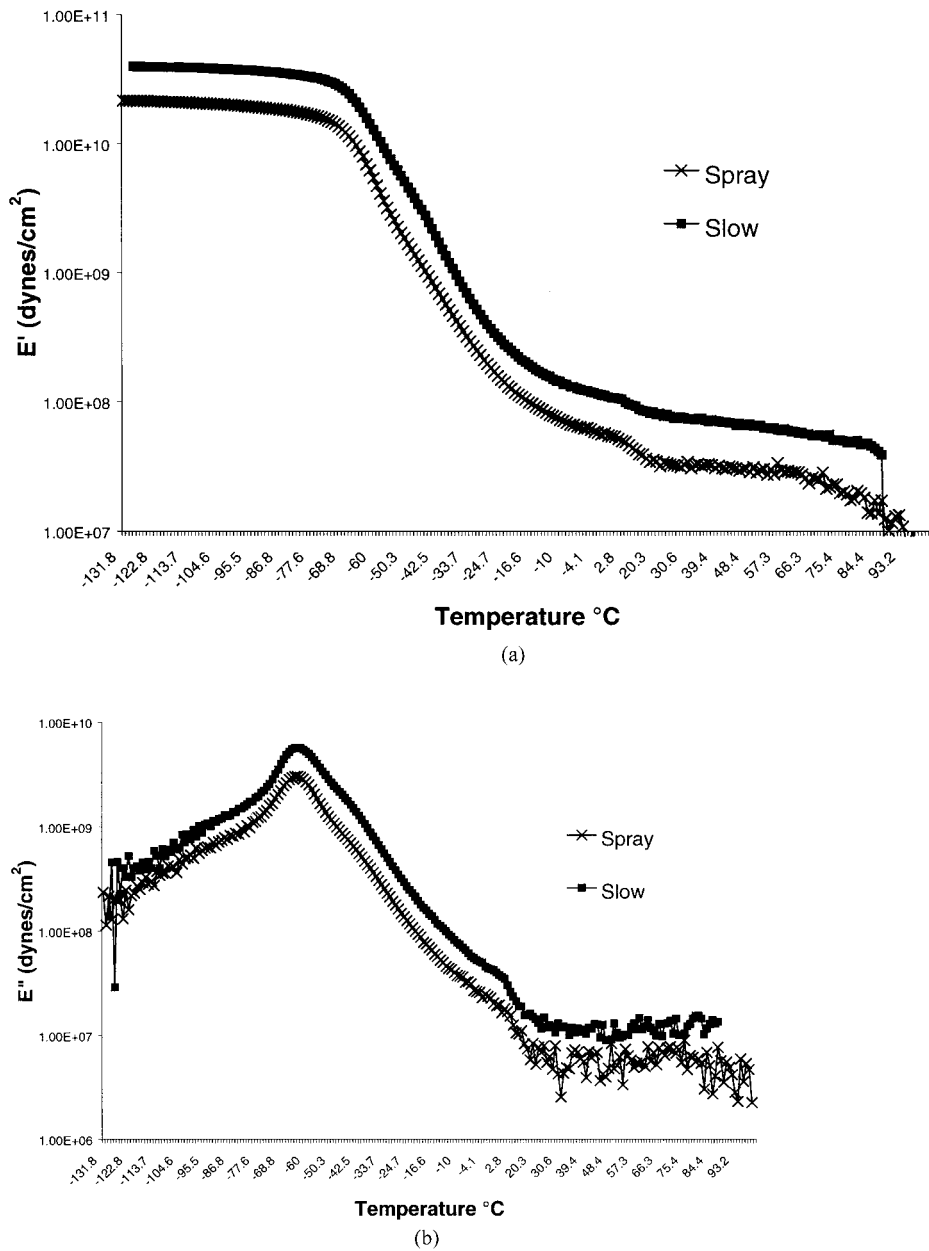


Fig. 2. (a)  $E'$ , (b)  $E''$ , (c)  $\tan \delta$  of PS-PIB-PS films formed by different processing methods.

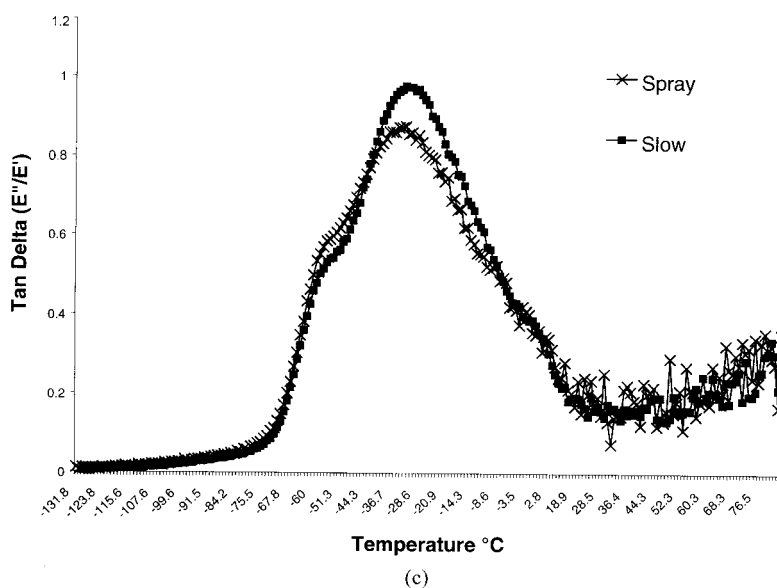


Fig. 2. (Continued).

not affect the  $T_g$  or the magnitude of the glass transition ( $E''$  maxima) of the PIB matrix.  $E''$  of the sulfonated polymer is significantly higher than the unmodified polymer at temperatures above  $0^\circ\text{C}$ . Fig. 3c shows  $\tan \delta$  for the two polymers. The sulfonated PS-PIB-PS exhibits a greatly reduced  $\tan \delta$  magnitude.  $\tan \delta$  maxima for the sulfonated polymer appears to correlate with the low-temperature shoulder of the PS-PIB-PS  $\tan \delta$  peak. The shape of the  $\tan \delta$  curve for the PS-PIB-PS ionomer appears to be reversed from the unmodified copolymer. That is, rather than the presence of the low-temperature shoulder preceding the  $\tan \delta$  maxima as observed for PS-PIB-PS, the sulfonated polymer exhibits the prominent  $\tan \delta$  transition at approximately  $-57^\circ\text{C}$ , corresponding with the low-temperature shoulder of the unmodified copolymer, followed by a higher temperature shoulder at approximately  $-45^\circ\text{C}$ . Although we believe that the lower temperature  $\tan \delta$  transition is the result of the PIB  $T_g$ , more studies are required to determine the molecular relaxation corresponding to the higher temperature  $\tan \delta$  transition. Mani et al. [8] reported similar results for copolymer ionomers prepared by sulfonation of the PS blocks of PS-poly(ethylene-*alt*-propylene) (PEP). The authors concluded that the enhancement of the high-temperature

modulus is the result of association and hydrogen bonding of the sulfonic acid groups [8].

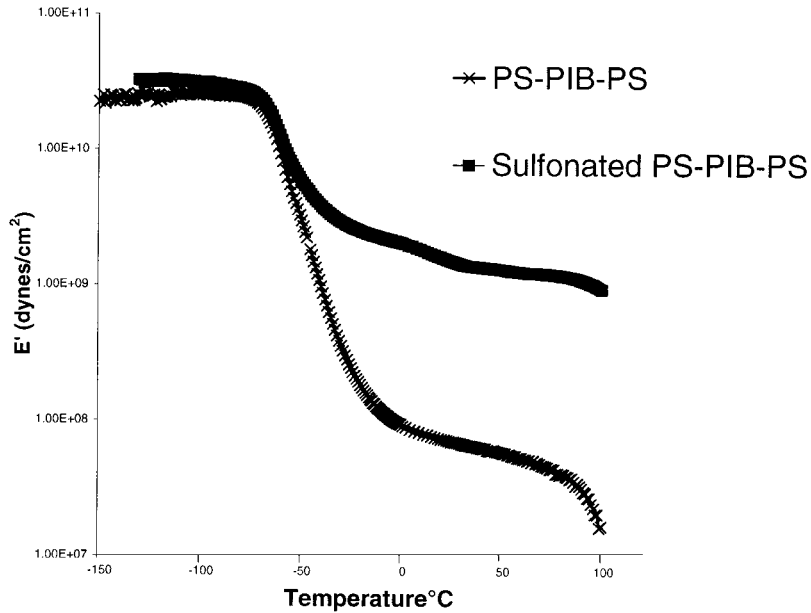
### 3.2. Sorption studies

Solvent sorption and permeation studies were conducted to ascertain the effect of morphology and sulfonation of PS-PIB-PS on the ability of the polymer to absorb and transport water. Details of experimental methods used to measure permeation and calculation of diffusion coefficients are discussed elsewhere [9,10]. Average solubility and diffusion coefficients are shown in Table 1. The hydrophobic nature of PS-PIB-PS is reflected in the solubility measurements. The unmodified copolymer exhibited a low value of water sorption, and no transport of water vapor through the film was detected. Sulfonation of approximately 20 mol% of the styrene monomers resulted in a threefold increase in average water solubility. This observation is consistent with previous findings that ionic content in polymers up to 15 mol% typically results in water sorption between 10 and 40 wt.% of sample dry weight [11]. Increasing ion content in polymers results in greater water sorption capacity [12]. This capability enables transport of ions and small molecules through a membrane.

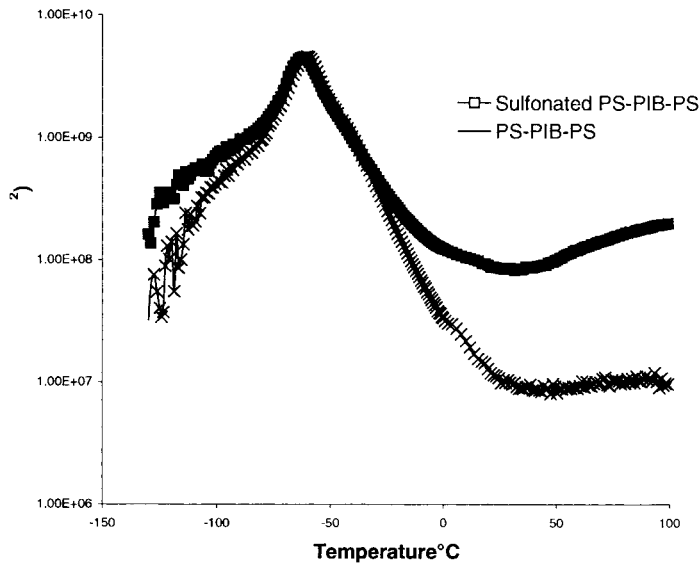
### 3.3. Characterization of microstructure

The morphology in both modified and unmodified PS-PIB-PS triblocks was studied using a combination of SAXS and TEM. TEM results, shown in Fig. 4a and

b, reveal a microphase-separated morphology in both the unmodified and sulfonated PS-PIB-PS triblocks. In the unmodified copolymers, the morphology is typical of self-assembled cylindrical systems and displays considerable long-range order (Fig. 4a). The



(a)



(b)

Fig. 3. (a)  $E'$  of PS-PIB-PS of copolymer; (b)  $E''$  and (c)  $\tan \delta$  of unmodified PS-PIB-PS copolymer and ionomer.

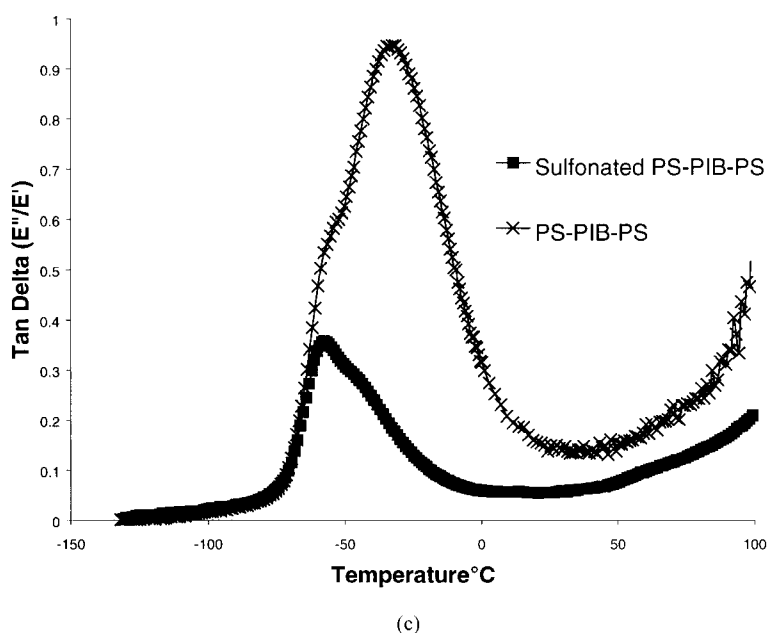


Fig. 3. (Continued).

Table 1  
Sorption and permeation of PS-PIB-PS and ionomer

Polymer/evaporation rate	Average solubility, $S$ (g water/g sample)	Diffusion coefficient, $D$ (cm <sup>2</sup> /s)	Permeability, $P$ (cm <sup>2</sup> × g water/g sample × s)
PS-PIB-PS/fast	0.0547	Too small to measure	Too small to measure
Ionomer/fast	0.1336	$3.5024 \times 10^{-7}$	$4.6793 \times 10^{-8}$
Ionomer/inter.	0.1636	$8.7838 \times 10^{-8}$	$1.4731 \times 10^{-8}$
Ionomer/slow	0.1211	$1.1491 \times 10^{-7}$	$1.3916 \times 10^{-8}$

SAXS curves for these materials, shown in Fig. 5, show evidence of long-range order as well. Scattering peaks occur at positions that are multiples of  $\sqrt{3}$ , 2,  $\sqrt{7}$ , and 3 times the position of the primary reflection, indicating that the copolymer forms a hexagonally packed cylindrical morphology. The degree of long-range order is found to be somewhat dependent on processing technique, increasing as the time for film casting increases, as evidenced by sharper scattering peaks and more prevalent high-order reflections (Fig. 6). The most significant change to the morphology occurs as a result of sulfonating the PS block. After sulfonation, the long-range order of the copolymer is severely disrupted. The electron micrograph, Fig. 4b, shows that the sulfonated triblock forms

cylinders that order only locally. The SAXS data also show a loss of long-range order, as evidenced by the broadening of the scattering peaks, and the lack of clearly defined scattering peaks at higher  $Q$  values (Fig. 7). The disruption of long-range order upon sulfonation is similar to effects observed in other triblock thermoplastic elastomer systems and has been previously reported [1,13].

#### 4. Conclusions

The morphology and viscoelastic properties of PS-PIB-PS triblock copolymers were studied with respect to film processing and sulfonation of approximately

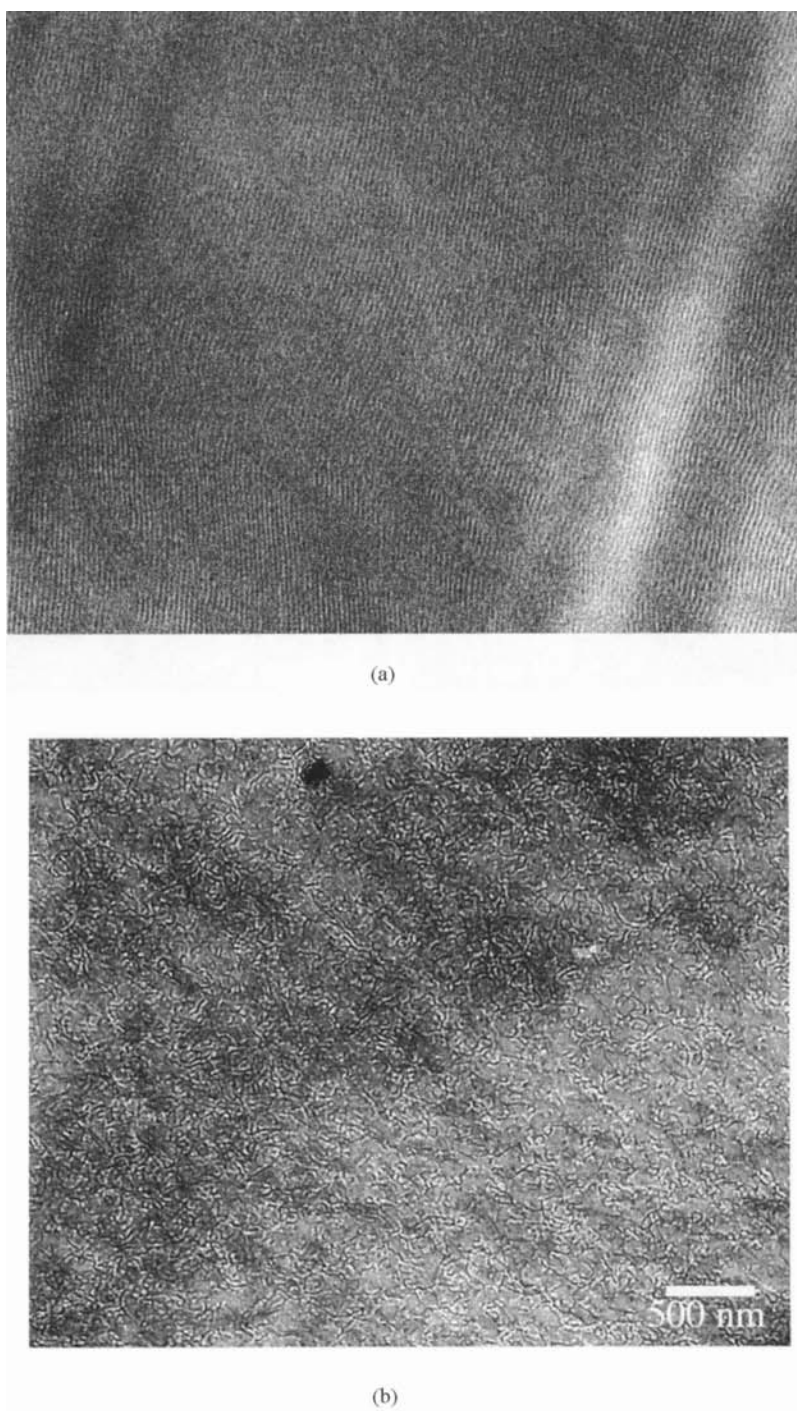


Fig. 4. (a) Unmodified and (b) sulfonated PS-PIB-PS film formed under fast evaporation conditions. PS phase was stained by  $\text{RuO}_4$  and appears as the dark regions.



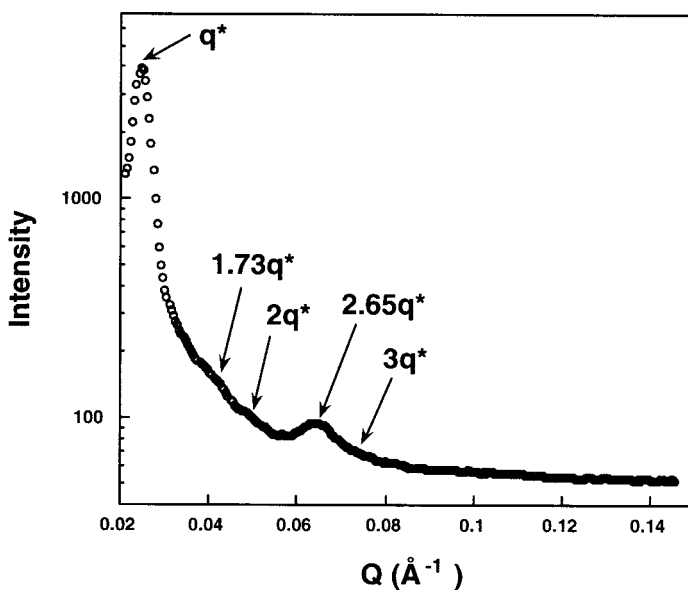


Fig. 5. SAXS intensity versus scattering vector,  $Q$ , for PS-PIB-PS triblock, slow casting condition. Peaks occur in the sequence  $1, \sqrt{3}, 2, \sqrt{7}, 3$  times the position of the primary scattering peak,  $q^*$ . The primary scattering peak occurs at  $q^* = 0.0245 \text{ \AA}^{-1}$ .

20 mol% of the styrene monomers. TEM and SAXS studies confirmed that the copolymers exhibit phase-segregated cylindrical domain morphology and indicated that slow evaporation rates enhanced long-range

order of the PS domains, while sulfonation greatly perturbed the morphology. Sulfonation of the styrene blocks had a dramatic effect on dynamic mechanical properties. Ionomers of PS-PIB-PS exhibited greatly

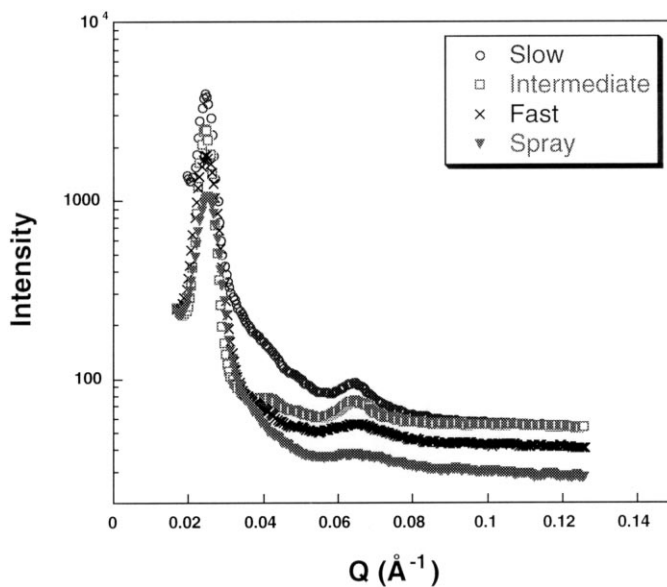


Fig. 6. SAXS intensity versus scattering vector,  $Q$ , for PS-PIB-PS triblocks, different casting conditions. For all conditions, the primary scattering peak occurs at  $q^* = 0.0245 \text{ \AA}^{-1}$ .

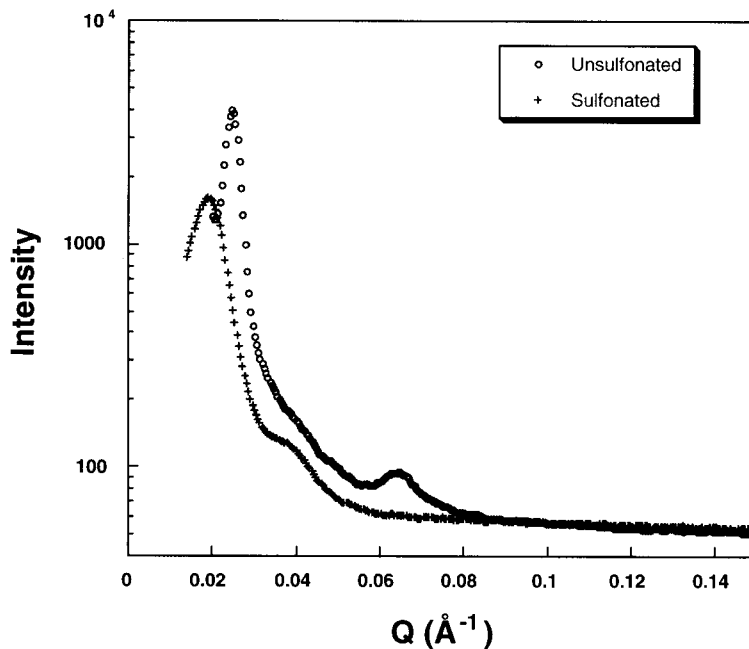


Fig. 7. SAXS intensity versus scattering vector,  $Q$ , for sulfonated and unsulfonated PS-PIB-PS triblocks, slow casting condition. The primary scattering vector in the sulfonated system,  $q_s^*$ , occurs at a lower value than for the unsulfonated system.

increased rubbery plateau  $E'$  and a dramatic reduction in  $\tan \delta$  magnitude. These observations are believed to be related to associations of the sulfonic acid groups resulting in a crosslinking effect. Sulfonation did not affect the  $T_g$  of the PIB matrix, or the magnitude of the PIB low-temperature relaxation as shown in the  $E''$  data. Sorption and permeation studies showed that the ionomer exhibited significantly improved water transport properties. Future studies are planned to specifically address the morphological features in the ionomers with respect to sulfonation levels and counter-ion substitution.

## References

- [1] X. Lu, W.P. Steckle Jr., R.A. Weiss, *Macromolecules* 26 (1993) 6525.
- [2] R.A. Weiss, A. Sen, L.A. Pottick, C.L. Willis, *Polym. Commun.* 31 (1990) 220.
- [3] D.A. Mountz, D.A. Reuschle, L.B. Brister, R.F. Storey, K.A. Mauritz, *ACS Polym. Preprints* 39 (1997) 383.
- [4] L.H. Sperling, *Introduction to Physical Polymer Science*, 2nd Edition, Wiley, New York, 1992, p. 367.
- [5] D.A. Reuschle, D.A. Mountz, B. Brister, C.L. Curry, K.A. Shoemaker, R.F. Storey, K.A. Mauritz, *ACS Polym. Preprints* 39 (1997) 381.
- [6] G. Kim, M. Libera, *Macromolecules* 31 (1998) 2569.
- [7] G. Kim, M. Libera, *Macromolecules* 31 (1998) 2670.
- [8] S. Mani, R.A. Weiss, C.E. Williams, S.F. Hahn, *Macromolecules* 32 (1999) 3663.
- [9] C.B. Billing, A.P. Bentz, in: R. Sager, A.P. Nielsen (Eds.), *Performance of Protective Clothing: Second Symposium of ASTM STP*, American Society for Testing and Materials, Philadelphia, PA, 1988, pp. 226–235.
- [10] S. Pauly, in: J. Brandrup, E.H. Immergut (Eds.), *Polymer Handbook*, 3rd Edition, Wiley, New York, 1989, pp. 435–439.
- [11] H.L. Yeager, A.A. Gronowski, in: M.R. Tant, K.A. Mauritz, G.L. Wilkes (Eds.), *Ionomers Synthesis, Structure, Properties and Applications*, Blackie Academic and Professional, New York, 1997, p. 333.
- [12] A. Eisenberg, J-S. Kim, *Introduction to Ionomers*, Wiley, New York, 1998, pp. 132–133.
- [13] R.A. Weiss, A. Sen, L.A. Pottick, C.L. Willis, *Polymer* 32 (1991) 2785.